Session: Ultra-High Magnetic Field Diffusion, Perfusion & Functional MRI

Speaker: Wietske van der Zwaag wietske.vanderzwaag@epfl.ch

Highlights

- Functional MRI benefits in two ways from increases in field strength as both image SNR and BOLD signal changes increase, leading to large increases in sensitivity.
- Drawbacks or points of attention are the increased susceptibility induced distortions, B_0/B_1 inhomogeneities and physiological noise contributions.

Applications of ultra-high field to study human brain function

Target audience:

Physicists and/or neuroscientists starting to use an ultra-high field scanner (≥7T) for their fMRI experiments and those interested in doing so in the future.

Outcome/objectives:

Following this lecture, those in the audience should have a good understanding of the field strength dependence of the MR parameters of importance for fMRI. The lecture should help listeners to understand which studies might benefit from the use of an ultra-high field system and how, and also, which studies would not stand to gain much from an increase in B_0.

Effects of field strength on fMRI

Many MR-parameters are to some extent field strength dependent. In the case of fMRI, the single most important change is the increased sensitivity to susceptibility differences, which leads to a near-linear increase in BOLD response amplitude with field strength [1–3]. While this increased BOLD signal is undoubtedly a benefit to fMRI, the accompanying increase in susceptibility-induced distortions at air-water interfaces is rather more problematic. Other notable changes are the increase in available magnetisation[4], a decrease in $T_2^{(*)}$, an increase in physiological noise contributions[5], an increase in rf-power deposition and, somewhat less importantly, longer T_1 values for both grey and white matter and an increase in B_1 inhomogeneities. These points will all be discussed, with some more emphasis on the aspects that have a direct impact on fMRI acquisitions.

The increase in task-induced BOLD-signal changes was first described for a change in field strengths from 1.5 to 4T[3] and has since been confirmed for a change in field strength from 4 to 7T[2] and for the common field strengths of 1.5, 3 and 7T[1]. The BOLD signal arises from local field inhomogeneities caused by magnetic susceptibility differences between deoxyhaemoglobin-rich blood in capillaries and venous vessels and the surrounding tissue, which scale linearly with field strength. The resulting increase in BOLD contrast is of great benefit for functional MRI studies and can be exploited to improve the spatial resolution, or

reduce the number of trials/participants required to demonstrate robust activation. The increase in BOLD signal changes is roughly linear with magnetic field[1], motivating the use of ever higher field strengths for fMRI.

The increase in susceptibility differences simultaneously results in increased susceptibility-induced distortions and through-slice de-phasing. These are best countered through an increase in spatial resolution, which reduces the effect of within-voxel gradients[6]. Many groups have demonstrated good echo planar image quality provided limited voxel sizes are used. For an example, see the echo planar image in Figure 1, which shows fine anatomical detail and limited geometrical distortions. Geometric distortions can also be reduced post-acquisition through corrections based on the use of a field map[7] or other reference data[8]. Signal lost through through-slice de-phasing cannot be recovered with post-processing methods – only by changes in image acquisition strategies[910].

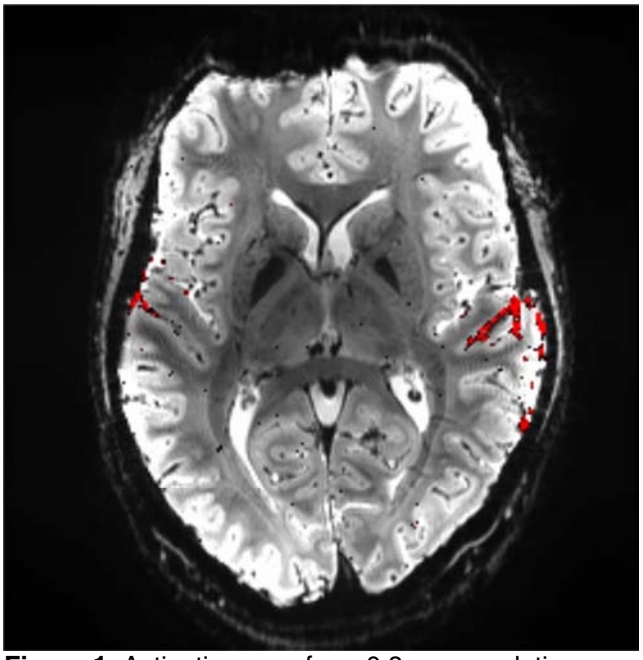

Figure 1. Activation map from 0.8 mm resolution gradient echo EPI data for an auditory task shown overlaid on the average of the planar imaging volumes it was generated from.

While the increase in available magnetization and resulting higher SNR[4] can be seen straightforwardly as an advantage, the reduction in transverse relaxation times T_2 and T_2^* is both a limitation and an advantage. Faster relaxation means shorter echo trains can be acquired while avoiding blurring introduced by signal decay during the echo planar readout[11], but also mean that more slices can be acquired in a limited TR while keeping $TE \approx T_2^*$; which is important for applications where whole-brain coverage is required or coveted, such as resting state fMRI[12]. An additional advantage for ultra-high field fMRI is provided in the increased shortening of the venous T_2^* compared to the tissue T_2^*, effectively reducing venous signal and thus false positive BOLD changes from draining veins[1,13].

Cardiac and respiratory processes, which are unavoidable in fMRI, as well as subject motion, create temporal signal fluctuations in the brain, which are usually referred to as 'physiological noise'. Since the physiological fluctuations represent a multiplicative modulation of the image signal, their amplitude scales with the MR image intensity and thus, for a given voxel size, with field strength[5]. A reduced voxel size can make the loss in BOLD sensitivity due to the increased signal instability smaller[5,14]. Alternatively, the lost BOLD sensitivity can be recovered post-acquisition, either by acquiring at high resolution and subsequent smoothing[15] or via the removal of signals correlated with cardiac and respiratory processes using methods such as RETROICOR[16] or reference-region based strategies[17,18].

Increased B_1-inhomogeneity due to the shorter wavelength is not a significant problem in gradient-echo based EPI, but can dramatically alter T_2-weighting throughout the image in spin-echo (SE)-EPI[19]. At the same time, SAR limitations, which do not tend to limit gradient-echo EPI acquisitions, can seriously reduce the number of slices that can be acquired in SE-EPI because of the high-intensity inversion pulse. There is thus a need for B_1-inhomogeneity insensitive, low SAR rf-pulses for successful SE-EPI at 7T. Adiabatic pulses, while not sensitive to B_1-inhomogeneities, yield too high SAR levels for use in multi-slice fMRI[11]. PINS rf-pulses[19] provide a low-power alternative and a good solution is also supplied by parallel transmit techniques[20], provided the necessary hardware is available.

Neuroscience studies using UHF fMRI

While there are many studies emphasizing the benefits of the use of UHF in a range of brain regions (for example: occipital cortex[2], motor cortex[1], amygdala[21], hippocampus[22], or more extended brain regions[12,23]), the number of publications with a purely neuroscientific objective has been rather limited until very recently (Figure 2).

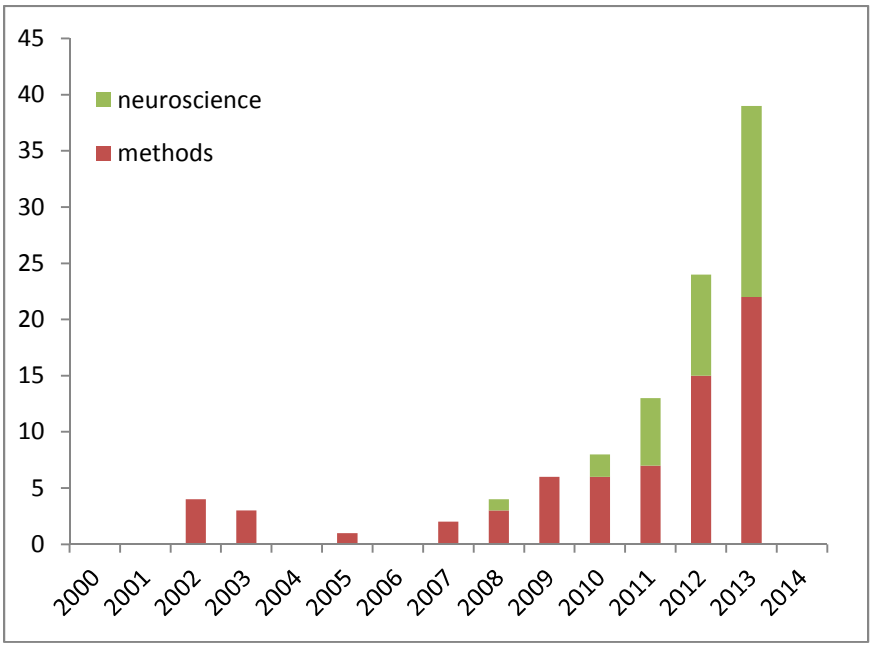

Figure 2. 7T fMRI papers published in peer-reviewed journals per year, divided into methods and neuroscience focused studies.

As can be concluded from the previous section, high-resolution fMRI studies stand the most to gain from UHF. Most applied UHF fMRI studies therefore use the high spatial resolution to specifically address a neuroscientific question that cannot be addressed at lower resolution. Although it should be noted that while nearly all 'neuroscience' studies were performed at <2mm isotropic resolution, only very few used a voxel size <1mm^3, which has been demonstrated as feasible in several methods papers[24–26]. In the following, a few examples will be given of recent neuroscience-driven ultra-high field fMRI studies.

The earliest applications of 7T fMRI were in the already relatively well-studied visual cortex. An extremely high in-plane spatial resolution of 0.5mm was reached in a multi-shot, SE-EPI acquisition of a single 3mm slice. With this very high resolution protocol, Yacoub et al were able to demonstrate that they could map ocular dominance columns[11] and, in a follow up study, demonstrated the presence of orientation columns in human VI[27]

Due to cortical folding, fMRI outside VI benefits from isotropic voxel sizes, as used for example in somatotopic mapping of the primary sensory cortex[2829]. In these studies, a map spanning several Brodmann regions, distributed over two flanks and the crown of a sulcus, was successfully mapped with a GRE-EPI of 1.5 mm isotropic resolution.

Applications of 7T fMRI for the mapping of higher cognitive functions have been done more recently too, with a good example published in Science last September[30]. High-resolution 7T fMRI (1.98*1.98*2 mm) was used to map neural representations of 'numerosity' in a small region in the parietal association cortex using neural models similar to those applied in the visual cortex.

Conclusions

7T fMRI benefits from high SNR and BOLD sensitivity, which can be traded for spatial resolution to limit the adverse effects of high field strength, such as susceptibility induced distortions and physiological noise contamination. Very recently, a dramatic increase in neuroscience applications for high-resolution, ultra-high field fMRI has been noted, starting a field which is expected to further expand in the coming years.

References

1. Van der Zwaag, W. *et al.* fMRI at 1.5, 3 and 7 T: characterising BOLD signal changes. *Neuroimage* **47,** 1425–1434 (2009).
2. Yacoub, E. *et al.* Imaging brain function in humans at 7 Tesla. *Magn. Reson. Med. Off. J. Soc. Magn. Reson. Med. Soc. Magn. Reson. Med.* **45,** 588–594 (2001).
3. Turner, R. *et al.* Functional mapping of the human visual cortex at 4 and 1.5 tesla using deoxygenation contrast EPI. *Magn. Reson. Med. Off. J. Soc. Magn. Reson. Med. Soc. Magn. Reson. Med.* **29,** 277–279 (1993).
4. Edelstein, W. A., Glover, G. H., Hardy, C. J. & Redington, R. W. The intrinsic signal-to-noise ratio in NMR imaging. *Magn. Reson. Med. Off. J. Soc. Magn. Reson. Med. Soc. Magn. Reson. Med.* **3,** 604–618 (1986).
5. Triantafyllou, C. *et al.* Comparison of physiological noise at 1.5 T, 3 T and 7 T and optimization of fMRI acquisition parameters. *Neuroimage* **26,** 243–250 (2005).
6. Speck, O., Stadler, J. & Zaitsev, M. High resolution single-shot EPI at 7T. *Magma New York N* **21,** 73–86 (2008).
7. Jezzard, P. & Balaban, R. S. Correction for geometric distortion in echo planar images from B0 field variations. *Magn. Reson. Med. Off. J. Soc. Magn. Reson. Med. Soc. Magn. Reson. Med.* **34,** 65–73 (1995).
8. Oh, S.-H. *et al.* Distortion correction in EPI at ultra-high-field MRI using PSF mapping with optimal combination of shift detection dimension. *Magn. Reson. Med. Off. J. Soc. Magn. Reson. Med. Soc. Magn. Reson. Med.* **68,** 1239–1246 (2012).
9. Glover, G. H. 3D z-shim method for reduction of susceptibility effects in BOLD fMRI. *Magn. Reson. Med. Off. J. Soc. Magn. Reson. Med. Soc. Magn. Reson. Med.* **42,** 290–299 (1999).

10. Van der Zwaag, W., Da Costa, S. E., Zürcher, N. R., Adams, R. B., Jr & Hadjikhani, N. A 7 tesla FMRI study of amygdala responses to fearful faces. *Brain Topogr.* **25,** 125–128 (2012).
11. Yacoub, E., Shmuel, A., Logothetis, N. & Uğurbil, K. Robust detection of ocular dominance columns in humans using Hahn Spin Echo BOLD functional MRI at 7 Tesla. *Neuroimage* **37,** 1161–1177 (2007).
12. De Martino, F. *et al.* Whole brain high-resolution functional imaging at ultra high magnetic fields: an application to the analysis of resting state networks. *Neuroimage* **57,** 1031–1044 (2011).
13. Gati, J. S., Menon, R. S., Ugurbil, K. & Rutt, B. K. Experimental determination of the BOLD field strength dependence in vessels and tissue. *Magn. Reson. Med. Off. J. Soc. Magn. Reson. Med. Soc. Magn. Reson. Med.* **38,** 296–302 (1997).
14. Hutton, C. *et al.* The impact of physiological noise correction on fMRI at 7 T. *Neuroimage* **57,** 101–112 (2011).
15. Triantafyllou, C., Hoge, R. D. & Wald, L. L. Effect of spatial smoothing on physiological noise in high-resolution fMRI. *Neuroimage* **32,** 551–557 (2006).
16. Glover, G. H., Li, T. Q. & Ress, D. Image-based method for retrospective correction of physiological motion effects in fMRI: RETROICOR. *Magn. Reson. Med. Off. J. Soc. Magn. Reson. Med. Soc. Magn. Reson. Med.* **44,** 162–167 (2000).
17. Jorge, J., Figueiredo, P., van der Zwaag, W. & Marques, J. P. Signal fluctuations in fMRI data acquired with 2D-EPI and 3D-EPI at 7 Tesla. *Magn. Reson. Imaging* **31,** 212–220 (2013).
18. Bianciardi, M., van Gelderen, P., Duyn, J. H., Fukunaga, M. & de Zwart, J. A. Making the most of fMRI at 7 T by suppressing spontaneous signal fluctuations. *Neuroimage* **44,** 448–454 (2009).
19. Norris, D. G., Koopmans, P. J., Boyacioğlu, R. & Barth, M. Power Independent of Number of Slices (PINS) radiofrequency pulses for low-power simultaneous multislice excitation. *Magn. Reson. Med. Off. J. Soc. Magn. Reson. Med. Soc. Magn. Reson. Med.* **66,** 1234–1240 (2011).
20. De Martino, F. *et al.* Spin echo functional MRI in bilateral auditory cortices at 7 T: an application of B_1 shimming. *Neuroimage* **63,** 1313–1320 (2012).
21. Sladky, R. *et al.* High-resolution functional MRI of the human amygdala at 7 T. *Eur. J. Radiol.* **82,** 728–733 (2013).
22. Theysohn, N. *et al.* Memory-related hippocampal activity can be measured robustly using FMRI at 7 tesla. *J. Neuroimaging Off. J. Am. Soc. Neuroimaging* **23,** 445–451 (2013).
23. Hahn, A. *et al.* Comparing neural response to painful electrical stimulation with functional MRI at 3 and 7 T. *Neuroimage* **82,** 336–343 (2013).
24. Salomon, R., Darulova, J., Narsude, M. & van der Zwaag, W. Comparison of an 8-Channel and a 32-Channel Coil for High-Resolution fMRI at 7 T. *Brain Topogr.* (2013). doi:10.1007/s10548-013-0298-6
25. De Martino, F. *et al.* Cortical depth dependent functional responses in humans at 7T: improved specificity with 3D GRASE. *PloS One* **8,** e60514 (2013).
26. Poser, B. A., Koopmans, P. J., Witzel, T., Wald, L. L. & Barth, M. Three dimensional echo-planar imaging at 7 Tesla. *Neuroimage* **51,** 261–266 (2010).
27. Yacoub, E., Harel, N. & Ugurbil, K. High-field fMRI unveils orientation columns in humans. *Proc. Natl. Acad. Sci. U. S. A.* **105,** 10607–10612 (2008).
28. Martuzzi, R., van der Zwaag, W., Farthouat, J., Gruetter, R. & Blanke, O. Human finger somatotopy in areas 3b, 1, and 2: A 7T fMRI study using a natural stimulus. *Hum. Brain Mapp.* (2012). doi:10.1002/hbm.22172

29. Sanchez-Panchuelo, R. M., Francis, S., Bowtell, R. & Schluppeck, D. Mapping human somatosensory cortex in individual subjects with 7T functional MRI. *J. Neurophysiol.* **103,** 2544–2556 (2010).
30. Harvey, B. M., Klein, B. P., Petridou, N. & Dumoulin, S. O. Topographic representation of numerosity in the human parietal cortex. *Science* **341,** 1123–1126 (2013).